NeuroImage: Clinical 27 (2020) 102294

Contents lists available at ScienceDirect

NeuroImage: Clinical

journal homepage: www.elsevier.com/locate/ynicl

Characterizing the heterogeneous metabolic progression in idiopathic REM sleep behavior disorder

Xianhua Han[a,†], Ping Wu[a,†], Ian Alberts[b], Hucheng Zhou[j], Huan Yu[c], Panagiotis Bargiotas[d,n], Igor Yakushev[e], Jian Wang[c], Guenter Höglinger[f], Stefan Förster[e,p], Claudio Bassetti[d], Wolfgang Oertel[g], Markus Schwaiger[l], Sung-Cheng Huang[h], Paul Cumming[b,i], Axel Rominger[b], Jiehui Jiang[j,*], Chuantao Zuo[a,k,m,*], Kuangyu Shi[b,o]

[a] PET Center, Huashan Hospital, Fudan University, Shanghai, China
[b] Department of Nuclear Medicine, University of Bern, Switzerland
[c] Department of Neurology, Huashan Hospital, Fudan University, Shanghai, China
[d] Department of Neurology, University Hospital Bern (Inselspital) and University of Bern, Bern, Switzerland
[e] Department of Nuclear Medicine, Technische Universität München, Munich, Germany
[f] Department of Neurology, Hannover Medical School, Germany
[g] Department of Neurology, University of Marburg, Germany
[h] Department of Molecular and Medical Pharmacology, UCLA, Los Angeles, USA
[i] School of Psychology and Counselling and IHBI, Queensland University of Technology, Brisbane, Australia
[j] Key Laboratory of Specialty Fiber Optics and Optical Access Networks, Joint International Research Laboratory of Specialty Fiber Optics and Advanced Communication ,Shanghai Institute for Advanced Communication and Data Science, Shanghai University, Shanghai, China
[k] Human Phenome Institute, Fudan University, Shanghai, China
[l] Klinikum r. d. Isar, Technische Universität München, Munich, Germany
[m] Institute of Functional and Molecular Medical Imaging, Fudan University, Shanghai, China
[n] Department of Neurology, Medical School, University of Cyprus, Nicosia, Cyprus
[o] Dept. Informatics, Technische Universität München, Munich, Germany
[p] Department of Nuclear Medicine, Klinikum Bayreuth, Germany

ARTICLE INFO

Keywords:
REM sleep behavior disorder
Parkinson's disease
PET
FDG
Conversion

ABSTRACT

Objective: Idiopathic rapid eye movement (REM) sleep behavior disorder (iRBD) is a prodromal stage of synucleinopathies such as Parkinson's disease (PD). Positron emission tomography (PET) with ^{18}F-FDG reveals metabolic perturbations, which are scored by spatial covariance analysis. However, the resultant pattern scores do not capture the spatially heterogeneous trajectories of metabolic changes between individual brain regions. Assuming metabolic progression occurs as a continuum from the healthy control (HC) condition to iRBD and then PD, we investigated spatial dynamics of progressively perturbed glucose metabolism in a cross-sectional study.

Methods: 19 iRBD patients, 38 PD patients and 19 HC subjects underwent ^{18}F-FDG PET. The images were spatially normalized, scaled to the global mean uptake, and automatically parcellated. We contrasted regional metabolism by group, and allocated the inferred progression to one of several possible trajectories. We further investigated the correlations between ^{18}F-FDG uptake and the disease duration in the iRBD and PD groups, respectively. We also explored relationships between ^{18}F-FDG uptake and the Unified Parkinson's Disease Rating Scale motor (UPDRS III) scores in the PD group.

Results: PD patients exhibited more extensive relative hyper- and hypo-metabolism than iRBD patients. We identified three dynamic metabolic trajectories, cross-sectional hypo- or hypermetabolism, cross-sectionally unchanged hypo- or hypermetabolism, cross-sectionally late hypo- or hypermetabolism, appearing only in the contrast of PD with iRBD. No correlation was found between relative ^{18}F-FDG metabolism and disease duration in the iRBD group. Regional hyper- and hypo-metabolism in the PD patients correlated with disease duration or clinical UPDRS III scores.

Conclusion: Cerebral metabolism changes heterogeneously in a continuum extending from HC to iRBD and PD

* Corresponding authors at: PET Center, Huashan Hospital, Fudan University, Shanghai, China.
E-mail addresses: jiangjiehui@shu.edu.cn (J. Jiang), zuochuantao@fudan.edu.cn (C. Zuo).
† Shared first author.

https://doi.org/10.1016/j.nicl.2020.102294
Received 21 September 2019; Received in revised form 10 May 2020; Accepted 11 May 2020
Available online 26 May 2020

groups in this preliminary study. The distinctive metabolic trajectories point towards a potential neuroimaging biomarker for conversion of iRBD to frank PD, which should be amenable to advanced pattern recognition analysis in future longitudinal studies.

1. Introduction

Idiopathic rapid eye movement (REM) sleep behavior disorder (iRBD) is a parasomnia characterized by loss of normal skeletal muscle atonia during REM sleep, leading to potentially harmful dream-enacting behaviors (Boeve, 2010). There is accumulating evidence that iRBD occurring in the absence of other clinically established neurological disorders is a prodromal phase of neurodegenerative synucleinopathies such as Parkinson's disease (PD), dementia with Lewy bodies (DLB), and multiple system atrophy (MSA) (Postuma et al., 2009; Iranzo et al., 2013; Iranzo et al., 2006). Indeed, meta-analysis shows the incidence of conversion to neurodegenerative disease is 34% at five years follow-up, increasing to 82% at 11 years and 97% at 14 years (Galbiati et al., 2019). Among these disorders, PD is the predominant late sequelus of iRBD (Iranzo et al., 2013; Schenck et al., 2013), ultimately occurring in some 43% of iRBD cases (Galbiati et al., 2019). Other studies have shown that 30–80% of PD patients present RBD symptoms, and that iRBD may precede the onset of PD motor symptoms by 3–13 years (Gagnon et al., 2002; Schrag et al., 2015; Iranzo et al., 2005), suggesting a shared or overlapping neurodegenerative pathway.

[^{18}F]-fluorodeoxyglucose (^{18}F-FDG) is widely used as a radiotracer for positron emission tomography (PET) imaging of cerebral metabolism *in vivo*; its trapping in brain gives a surrogate index of the metabolic rate for glucose, which is the main carbon source supporting cerebral energy metabolism. PET with ^{18}F-FDG findings can predict conversion to Alzheimer s disease (AD) and discriminate AD from other forms of dementia (Nestor et al., 2018; Drzezga et al., 2018). Similarly, ^{18}F-FDG PET reveals metabolic disturbances in PD (Eidelberg, 1992; Borghammer et al., 2010; Meles et al., 2017). Given the evident relationship between iRBD and PD, it might follow that ^{18}F-FDG PET could probe the metabolic patterns common to the two conditions. Indeed, voxelwise searches reveal regional patterns of altered relative metabolism in contrasts between controls, iRBD patients, and PD patients (Ge et al., 2015; Teune et al., 2010; Yong et al., 2007). However, the process of global intensity normalization raises certain caveats about the interpretation of such voxelwise comparisons of tracer uptake (Borghammer et al., 2009).

As an alternative to voxelwise contrasts, spatial covariance analysis can analyze metabolic patterns, whereby scores of specific disease-related patterns reflect the cerebral metabolic abnormalities of the particular neurodegenerative disorders (Eidelberg, 2009; Eckert et al., 2008; Ma et al., 2007). These scalar values are highly specific in distinguishing between PD and parkinsonian syndromes, thus aiding their differential diagnosis, which can be difficult when based only on initial clinical presentation (Tang et al., 2010). Using spatial covariance analysis algorithms, our research group has also identified specific RBD-related covariance pattern (RBDRP) and a PD-related covariance pattern (PDRP) in Chinese cohorts (Ge et al., 2015; Wu et al., 2013), which resembled the observations of other cohorts (Niethammer and Eidelberg, 2012). Owing to the unfitness of these spatial covariance analysis procedures to reveal distinct contributions of particular brain regions to the final score, a simple pattern score is insensitive to heterogeneous (anisotropic) progression of regional metabolic activities. The conventional method assumes that disease progression is proportional to the pattern vector images arising from the spatial covariance analysis. If one incorrectly assumes that trajectories of metabolic changes are linearly progressive in all brain regions, the analysis then suppresses any present anisotropic changes. Because spurious findings of consistently isotropic changes may not capture all details of the disease pathophysiology, we now propose an approach allowing regional differences in the trajectories of metabolic changes in progression from healthy controls (HC) to iRBD and then PD.

In this cross-sectional study, we mapped ^{18}F-FDG-PET uptake in a HC group, and in groups of iRBD or PD patients, aiming to explore the spatially heterogeneous metabolic trajectories occurring during the transition from HCs to iRBD and clinical PD.

2. Materials and methods

2.1. Participants

Three groups of age- and gender-matched participants were recruited from the Department of Neurology, Huashan Hospital, Fudan University, China for participation in the protocol, which was approved by the Research Ethics Committee of Huashan Hospital, Shanghai, China. All subjects provided written informed consent and took part in this study voluntarily.

A group of 38 PD patients (24 men; mean age 62.6 ± 7.6 years) was screened and clinically examined by two neurologists specializing in movement disorders before their inclusion in the study. PD diagnosis was according to the United Kingdom Brain Bank criteria (Hughes et al., 1992): Motor asymmetry, resting tremor, and clear response to levodopa must be present. Subjects with atypical parkinsonian features (excessive autonomic symptoms, oculomotor abnormalities) were excluded. A group of 19 iRBD patients (15 men; mean age 64.9 ± 5.6 years) were recruited, with diagnosis according to the third edition of the International Classification of Sleep Disorders criteria (Duchna, 2006; Montplaisir et al., 2010). A sleep disorder specialist diagnosed these patients based upon their clinical history and polysomnography (PSG). A group of 19 HC subjects (15 men; mean age 63.1 ± 7.5 years) were selected from among neurologically normal subjects undergoing an elective whole-body (including head) cancer-

Table 1
Demographic and clinical profiles of participants.

Variable	Healthy controls	iRBD	PD	*P*
Subjects (number)	19	19	38	—
Sex (male:female)	15:4	15:4	24:14	0.316[a]
Age (years)	63.1 ± 7.5	64.9 ± 5.6	62.6 ± 7.6	0.512[b]
Education (years)	—	12.6 ± 3.1	18.4 ± 7.6	0.002[c]
Duration of iRBD symptoms (months) after diagnosis		70.4 ± 43.7		
Duration of motor symptoms(months) after diagnosis	—		38.5 ± 24.3	
UPDRS III score at time of scanning	—	2.4 ± 2.1	18.4 ± 7.6	<0.0001[c]

Demographic and clinical data are presented as mean ± standard deviation.
[a] Chi-square for gender; [b] Analysis of variance; [c] Two-sample *t*-tests.

screening scan with ^{18}F-FDG PET. Only subjects without psychiatric disorder, and without use of psychotropic medication or hormone replacement within the prior six months, and without history of neurological disease, head injury, or alcohol abuse, were included in the HC group (Zhang et al., 2017). Any cases with occult ^{18}F-FDG-avid carcinoma on PET/CT examination were excluded. As described previously (Ge et al., 2015; Wu et al., 20142014), we excluded the possibility of RBD occurring in the HC groups by their response to the RBD-Single-Question Screen (RBDSQ) (Postuma et al., 2012). However, according to the RBDSQ, 21 of 38 (55.3%) PD patients had RBD symptoms, which is consistent with the relevant literature (Gagnon et al., 2002).

We evaluated motor symptoms of patients with PD and iRBD using the Unified Parkinson's Disease Rating Scale subscale (UPDRS III, items 18 to 31), which as administered at least 12 h after the cessation of antiparkinsonian medications. The clinical and demographic details of all included subjects are summarized in Table 1. Exclusion criteria for all participants included: (1) Significant general medical comorbidities, such as chronic obstructive pulmonary disease; (2) Central nervous system comorbidities such as cerebrovascular diseases, brain tumors, stroke, and encephalitis; (3) Metabolic diseases; (4) Primary psychiatric illnesses; (5) Previous abnormal findings on cranial magnetic resonance imaging (MRI) or computed tomography (CT); (6) Pregnancy and lactation. In addition, all PD patients and their caregivers were asked about patients' cognitive status. There were no amnestic reports of reduction in quality of life or hallucinations.

2.2. ^{18}F-FDG PET scanning

Before PET scanning, all participants were required to fast for at least six hours, but had free access to water. The PD patients withheld their medication for at least 12 h. PET scans were performed with a Siemens Biograph 64 HD PET/CT (Siemens, Germany) in three-dimensional (3D) mode. Emission data was recorded for ten minutes at 60 min after intravenous injection of 185 ± 25 MBq of ^{18}F-FDG (Wu et al., 2013). In addition, a low-dose CT transmission scan was carried out for attenuation correction. Data were reconstructed using 3D-ordered subset expectation maximization and corrected for random coincidences, scatter, and radioactive decay. All studies in the patient and HC subjects were conducted in a dimly lit room with minimal background noise.

2.3. Imaging processing

As a preliminary step, DICOM files were exported to a PC and converted into the *Analyze* format. Imaging data preprocessing was performed using Statistical Parametric Mapping (SPM5) software (Wellcome Department of Imaging Neuroscience, Institute of Neurology, London, UK) implemented in Matlab 7.2.0 (Mathworks Inc,

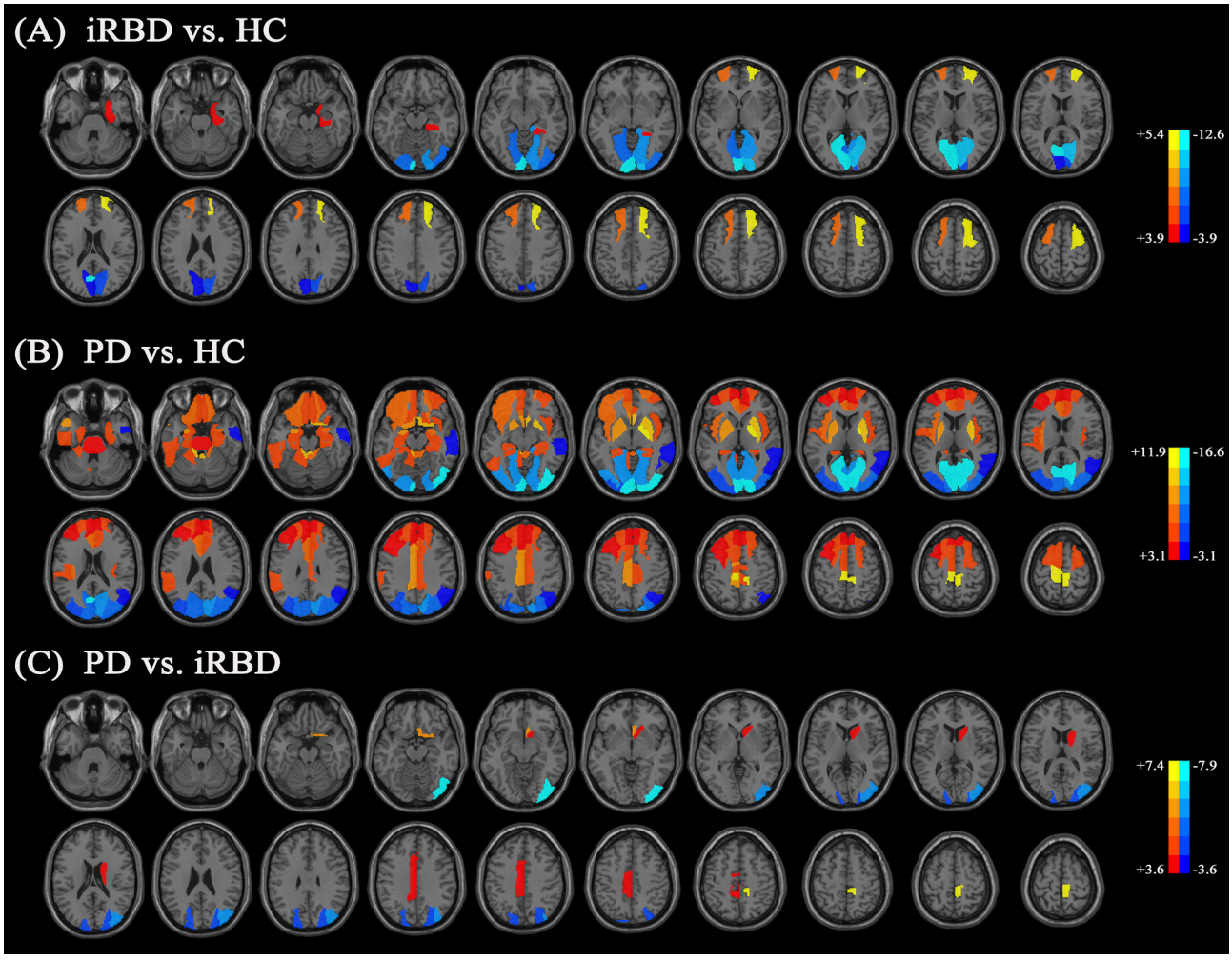

Fig. 1. (A) Brain regions with significantly (P < 0.0004) higher (yellow)/lower (blue) relative glucose metabolism in iRBD patients compared with controls. (B) Brain regions with significantly (P < 0.0004) higher (yellow)/lower (blue) relative glucose metabolism in PD patients compared with controls. (C) Brain regions with significantly (P < 0.0004) higher (yellow)/lower (blue) relative glucose metabolism in PD patients compared with iRBD patients. (For interpretation of the references to color in this figure legend, the reader is referred to the web version of this article.)

Table 2
Three dynamic metabolic patterns and the percentage of regional glucose metabolism of iRBD/PD patients to HCs.

Pattern	Labelled number	Labelled region	Percentage of iRBD to HC (%)	Percentage of PD to HC (%)
Cross-sectional				
Hypometabolism			Decrease	Decrease
	54	Occipital_Inf_R	−7.68 ± 5.49	−14.95 ± 3.93
Cross-sectionally unchanged				
Hypometabolism			Decrease	Decrease
	43	Calcarine_L	−12.62 ± 4.34	−16.61 ± 3.38
	44	Calcarine_R	−10.53 ± 4.72	−14.94 ± 3.82
	45	Cuneus_L	−5.10 ± 3.05	−8.69 ± 3.40
	46	Cuneus_R	−6.43 ± 2.94	−10.16 ± 3.58
	47	Lingual_L	−7.82 ± 3.62	−10.97 ± 3.23
	48	Lingual_R	−8.35 ± 4.01	−11.74 ± 3.24
Hypermetabolism			Increase	Increase
	3	Frontal_Sup_L	4.44 ± 2.71	5.27 ± 2.49
	4	Frontal_Sup_R	5.43 ± 2.92	4.66 ± 2.02
	40	Parahippocampus_R	3.92 ± 2.66	5.84 ± 2.93
Cross-sectionally late				
Hypometabolism			Decrease	Decrease
	49	Occipital_Sup_L	−3.02 ± 3.41	−7.77 ± 3.53
	50	Occipital_Sup_R	−3.28 ± 3.35	−8.06 ± 3.72
	52	Occipital_Mid_R	−3.68 ± 3.52	−9.83 ± 3.62
Hypermetabolism			Increase	Increase
	22	Olfactory_R	3.19 ± 4.38	9.32 ± 5.32
	33	Cingulum_Mid_L	3.78 ± 2.67	7.93 ± 3.25
	70	Paracentral_Lobule_R	2.95 ± 6.04	10.57 ± 6.40

Vaules are presented as mean ± standard deviation.

Sherborn, MA, USA). Scans from each subject were spatially normalized into Montreal Neurological Institute (MNI) space with linear and nonlinear 3D transformations. The spatially normalized PET images were then smoothed in 3D by a Gaussian filter of 10 mm full-width at half-maximum to reduce the individual anatomical variations and to increase the signal-to-noise ratio of the voxelwise data. The radioactivity images were scaled to the global mean activity in a whole brain mask to report relative regional glucose metabolism (Tang et al., 2010).

2.4. Data analysis

The spatially normalized and intensity-scaled PET images were aligned to an updated version of the automated anatomical labeling (AAL) atlas (Tzourio-Mazoyer et al., 2002) (provided by PMOD), parcellating the brain into 119 anatomical regions of interest (ROIs, denoted as AAL-119). For PD patients, scans from those with predominantly right-sided symptoms were flipped according to the UPDRS motor scores so that all hemispheres contralateral to the clinically more affected limbs appeared on the right side of the brain. For scans from normal controls and iRBD patients, flips were performed as described previously (Huang et al., 2019).

2.5. Characterizing metabolic trajectories

Regional relative metabolism was adjusted using the linear regression method to control the effects of age, gender, and education. Statistical analysis of relative metabolism in the HC, iRBD, and PD groups was performed using SPSS software (version 19.0) to search for patterns of metabolic change characterizing an inferred transition from the HC to iRBD and then PD. To identify the inferred progressive metabolic changes, we performed one-way analysis of variance (ANOVA) in conjunction with Bonferroni test to correct for multiple comparisons. To control the type 1 error, the statistical significance was set as $P < 0.0004(0.05/119)$. We further investigated the correlations between ^{18}F-FDG uptake in 119 regions and the disease duration in the iRBD and PD groups, respectively. Because iRBD patients have no or very mild motor impairment, we only investigated the correlation between ^{18}F-FDG uptake and UPDRS III scores in the PD group.

3. Results

3.1. Regional relative metabolic differences between iRBD patients and healthy controls

Compared with the HC group, iRBD patients exhibited significantly decreased glucose metabolism in the bilateral calcarine, cuneus, lingual gyrus and right inferior occipital gyrus ($P < 0.0004$), and relatively increased glucose metabolism in bilateral superior frontal gyrus and right parahippocampal gyrus ($P < 0.0004$). (Fig. 1A, Supplementary Materials_1 Table 1).

3.2. Regional metabolic differences between PD patients and HCs

Compared with the HC group, PD patients showed significantly decreased glucose metabolism in the bilateral calcarine, cuneus, lingual gyrus, superior occipital gyrus, middle occipital gyrus, inferior occipital gyrus, right angular gyrus and middle temporal gyrus ($P < 0.0004$), and relatively increased glucose metabolism in the bilateral frontal cortex, olfactory cortex, insula, anterior cingulate gyrus, middle cingulate gyrus, hippocampus, parahippocampal gyrus, amygdala, paracentral lobule, putamen, pallidum, Cerebellum3, left supplementary motor area, supramarginal gyrus, temporal pole (middle temporal gyrus), inferior temporal gyrus, Cerebellum45, Cerebellum8, and Vermis12, Vermis3, pons ($P < 0.0004$). (Fig. 1B, Supplementary Materials_1 Table 2).

3.3. Regional metabolic differences between PD patients and iRBD patients

Compared with the iRBD group, PD patients exhibited significantly decreased glucose metabolism in the bilateral superior occipital gyrus, right middle occipital gyrus and inferior occipital gyrus ($P < 0.0004$) and relatively increased glucose metabolism in the left middle cingulate gyrus, right olfactory cortex, paracentral lobule and caudate nucleus ($P < 0.0004$). (Fig. 1C, Supplementary Materials_1 Table 3).

3.4. Inferred dynamic patterns of altered cerebral glucose metabolism between the HC, iRBD, and PD groups

In the 119 brain regions, we identified three types of dynamic metabolic pattern across the HC, iRBD, and PD cohorts (Table 2). These were:

(1) Cross-sectional hyper- or hypometabolism: There was significant difference between any two groups of HC, iRBD and PD as well as a consistent trend of metabolic increase or decrease across the three cohorts. Cross-sectional hypometabolism was present in the right inferior occipital gyrus ($P < 0.0004$) (Fig. 2A). None of the 119 brain regions were cross-sectionally hypermetabolic.
(2) Cross-sectionally unchanged hypo- or hypermetabolism: There was significant difference between HC and iRBD, but no further difference between iRBD and PD. The cross-sectionally unchanged hypometabolism was found in the bilateral calcarine, cuneus and lingual gyrus ($P < 0.0004$) (Fig. 2 B-G). The cross-sectionally unchanged hypermetabolic regions were found in the bilateral superior frontal gyrus and right parahippocampal gyrus ($P < 0.0004$) (Fig. 2 H-J).
(3) Cross-sectionally late hypo- or hypermetabolism: There was significant difference between iRBD and PD but no difference between HC and iRBD. These hypometabolic regions were the bilateral superior occipital gyrus and right middle occipital gyrus ($P < 0.0004$) (Fig. 2 K-M). The relatively hypermetabolic regions were left middle cingulate gyrus, right olfactory cortex and paracentral lobule ($P < 0.0004$) (Fig. 2 N-P).

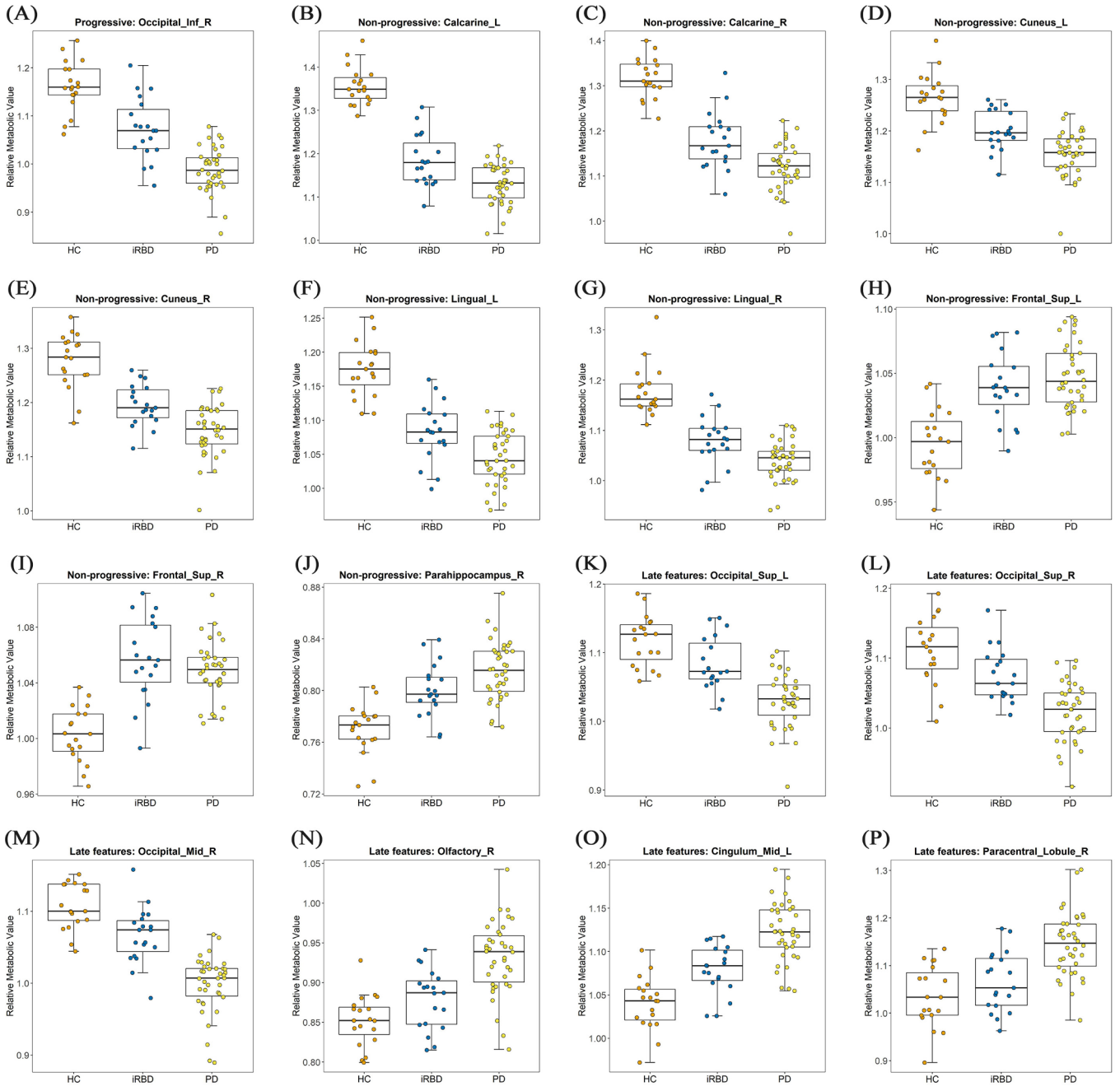

Fig. 2. The three categories of group differences in relative FDG uptake in representative brain regions ($P < 0.0004$). (A) The cross-sectional hypometabolism was present in the right inferior occipital gyrus. (B-G) The cross-sectionally unchanged hypometabolism was found in the bilateral calcarine, cuneus and lingual gyrus. (H-J) The cross-sectionally unchanged hypermetabolism was found in the bilateral superior frontal gyrus and right parahippocampal gyrus. (K-M) These hypometabolic regions in PD group were the bilateral superior occipital gyrus and right middle occipital gyrus. (N-P) The relatively hypermetabolic regions in PD group were right olfactory cortex, left middle cingulate gyrus, and right paracentral lobule.

3.5. Correlation of relative metabolic disturbances with disease duration or UPDRS III scores

No correlation was found between relative ^{18}F-FDG metabolism and disease duration in iRBD group. In PD group, a slight negative correlation between relative metabolic values and disease duration existed in the right middle frontal gyrus ($r = -0.351$, $P_{uncorrected} = 0.031$), and a positive correlation existed in the right posterior cingulate gyrus ($r = 0.334$, $P_{uncorrected} = 0.041$). Relative metabolic values correlated with UPDRS III scores negatively in the right middle temporal gyrus ($r = -0.336$, $P_{uncorrected} = 0.039$), and positively in the bilateral Cerebellum8 (Left: $r = 0.322$, $P_{uncorrected} = 0.049$; Right: $r = 0.321$, $P_{uncorrected} = 0.049$), and Vermis8 ($r = 0.383$, $P_{uncorrected} = 0.018$), Vermis9 ($r = 0.339$, $P_{uncorrected} = 0.037$), Vermis10 ($r = 0.352$, $P_{uncorrected} = 0.030$).

4. Discussion

We present in detail a comparison of relative glucose metabolism in brain regions of a HC group, and in iRBD and PD patient groups. Assuming a temporal sequence in the progression from a HC state to a transitional metabolic condition of iRBD and ultimately to PD, we explored for anisotropic metabolic changes, which might identify the key regional metabolic features of iRBD patients related to their later

conversion to PD. Thus, our objective was to identify a metabolic signature of synucleinopathy that precedes the onset of core motor symptoms. Our approach differs from earlier representations of disease-specific metabolic patterns, in that we do not require scalar covariance of cerebral metabolism in all afflicted regions, but allow anisotropy. This approach may better accommodate metabolic spatial heterogeneity of the disease process.

We find that the iRBD and PD patient groups both demonstrate extensive hypometabolism in occipital regions, together with relative hypermetabolism in the frontal regions. In comparison, PD patients had more widely distributed brain areas with metabolic changes. Among them, the areas of metabolic reduction involved more occipital lobe regions and some parts of temporal lobe, while the areas of relatively high metabolism involve more frontal lobe regions and many other cerebral or cerebellar regions. Thus, there is a gradual shift towards decreased metabolic rate in posterior cortical regions. Simultaneously, relative increased metabolism occurs in frontal and other regions. This pattern is consistent with previous reports (Ge et al., 2015; Ma et al., 2007; Wu et al., 20142014; Meles et al., 2018), and suggests a broad overlap of cerebrometabolic changes in iRBD and PD.

Similarly to the proposed "brain glucose metabolism heterogeneity" discerned in iRBD patients by a data-driven approach (Arnaldi et al., 2019), we infer in this cross-sectional study a variety of trajectories of regional cerebral metabolism in a conjectured transition from the HC group to iRBD and eventually to PD, which is considered as *sui generis* for synucleinopathies. Although there is a lack of difference in most of the 119 segmented brain regions, we found that some regions showed one of three change patterns: (1) "cross-sectional" hypo- or hypermetabolism, which means from the HC group to iRBD and finally to the PD group, there are consistent and continuous changes in brain metabolism. (2) "cross-sectionally unchanged" hypo- or hypermetabolism, which means brain metabolism changes in the early stage of the disease (i.e. iRBD) and remains stable in the following course of the disease. Or (3) "cross-sectionally late" hypo- or hypermetabolism, which means brain metabolism changes significantly only from iRBD stage to PD stage. Therefore, "cross-sectionally unchanged" hypo- or hypermetabolism can be regarded as the imaging feature of early diagnosis of PD, and "cross-sectionally late features" can be regarded as a marker of phenoconversion. The "cross-sectional" hypo- or hypermetabolism group show consistent and progressive metabolic changes from HC to iRBD to PD. We found that in any of the above change patterns, all areas with decreased glucose metabolism were located in the area of the occipital lobe mainly responsible for processing of visual information. Previous studies in iRBD and clinically diagnosed PD have stressed the importance of posterior cortical dysfunction to various non-motor symptoms such as visual hallucinations, cognitive impairment and poorer performance in the color discrimination test (Vendette et al., 2012; Mentis et al., 2002; Colloby et al., 2002; Vendette et al., 2011). Furthermore, a longitudinal SPECT study showed that the progression of regional cerebral blood flow deterioration in the parietal-temporal-occipital areas could reflect advancing neurodegeneration in iRBD patients, despite lack of worsening of non-motor impairments (Sakurai et al., 2014). Another follow-up [^{18}F]-FDG-PET study suggested that reduced baseline metabolism in the parietal-temporal-occipital areas in patients with probable RBD might predict eventual phenoconversion to DLB (Ota et al., 2016). We found that the "cross-sectionally unchanged" hypometabolism located in the medial parts of occipital lobe, such as the bilateral calcarine, cuneus and lingual gyrus is predictive of the development of synucleinopathies such as PD. However, the "cross-sectional" and "cross-sectionally late" hypometabolism located in the lateral parts of occipital lobe is indicative of progressive neurodegeneration. Our ongoing longitudinal studies in the iRBD patients could confirm the value of occipital hypometabolism as an imaging marker for diagnosis and progression assessment of PD or other synucleinopathies in their early stages.

We also found some areas with relatively increased glucose metabolism, which may be due to global normalization under the premise of absolute metabolism decline of cerebral cortex[18], although this concept has been debated (Ma et al., 2009; Borghammer et al., 2009). However, these changes still could be regarded as preclinical signs or progression indicators of synucleinopathies.

Our ROI analysis indicated no correlation between relative glucose metabolism in certain brain regions and disease duration or UPDRS III scores in iRBD patients and weak correlations in PD patients. The results are not surprising considering that the patients with iRBD have no parkinsonian motor signs and the time courses differ greatly for different patients developing from iRBD to PD. For PD patients, the negative correlation between disease duration and metabolism in the middle frontal gyrus may reflect the deterioration of the frontal function which is the main feature of the cognition of PD. In contrast, the posterior cingulate gyrus is mainly related to the cognitive function of AD and its metabolism may be relatively preserved in PD patients. The weak correlations between UPDRS motor scores and the cortical metabolism may be due to the fact that the cortical metabolism is more related to cognitive impairment but not to motor function.

This study was constrained by several limitations in addition to the relatively small sample size and the lack of longitudinal data which makes it possible to investigate the value of regional metabolic changes for predicting the clinical outcomes of RBD at single-subject level. Firstly, although this study used a ROI-and voxel-based analysis, the true pattern analyses (e.g., principal component analysis (PCA)) or cluster analyses were not presented. It still needs to investigate whether the pattern from PCA or cluster analyses were also efficient in our cases in the future. Secondly, while all PD patients and their caregivers were asked about patients' cognitive status, with no reports of cognitive decline which constrained their daily life, or the presence of hallucinations, no formal neuropsychological testing was undertaken for the PD group. Ideally, such information would be available. Future studies should consider possible relationships between metabolic patterns and cognition. However, cognitive assessments were available for all the RBD patients in this study (baseline and follow-up assessments). The follow-up assessments were done after PET examination and no clear cognitive impairments were found. Due to the diverse time points of the cognitive tests, we did not include the neuropsychological test data in the analysis. Future studies should encompass comprehensive cognitive testing in new studies in order to genuinely eliminate the possibility of MCI, and should also consider possible relationships between metabolic patterns and cognition. Thirdly, our HC participants were recruited without undergoing polysomnography, with exclusion of iRBD only through Single-Question screening. Although this screening has high sensitivity and specificity in diagnosing RBD (Postuma et al., 2012), we concede that screening of controls should properly have entailed a clinical confirmation. Fourthly, no partial volume correction (PVC) was not conducted in our study due to the lack of MRI data, which might hamper the results. Fifthly, we did not calculate the prodromal PD likehood ratio in this study because we did not have detailed clinical data of the iRBD patients, such as olfactory function scores. This will be addressed by ongoing studies. Sixthly, this study is not based on pattern analyses or cluster analyses. Instead, we did group-wise analysis between HC, iRBD and PD for the parcellated anatomical ROIs, and tried to explore the regional metabolic differences in a consecutive or progressive way, thus explorating of the spatially heterogeneous metabolic trajectories occurring during the transition from HCs to iRBD and clinical PD. Finally, the focus of this study was the relationship between iRBD and PD, which we take to be *sui generis* for synucleinopathy. Nevertheless, we are cognizant of the fact that iRBD can convert to other synucleinopathies such as dementia with Lewy bodies (DLB) and multiple system atrophy. These conditions should be included any future studies with long-term follow-up and a larger sample size.

In conclusion, this ^{18}F-FDG PET study using ROI-and voxel-based analysis replicates earlier findings of relative cerebral metabolic anomalies in a relatively limited sample of patients with iRBD and PD.

The considerable spatial overlap of relative hypermetabolism in frontal regions and hypometabolism in posterior occipital regions in both of our clinical groups suggests a common neurobiological process. Importantly, we characterized three spatially heterogeneous metabolic patterns from HC to iRBD and finally to PD, which might act as the early imaging feature or progression marker of the neurodegeneration process of PD. These preliminary findings are congruent with our hypothesis of an evolving anisotropically abnormal metabolic network proceeding from an early iRBD phase to later PD (Wu et al., 2014). Encouraged by these results, we are now undertaking longitudinal ^{18}F-FDG PET studies in larger cohorts, and will use advanced pattern recognition algorithms to confirm that the present markers can indeed predict and monitor the neurodegenerative progression of iRBD towards PD or other synucleinopathies.

5. Financial disclosure statement

No authors have received any funding from any institution, including personal relationships, interests, grants, employment, affiliations, patents, inventions, honoraria, consultancies, royalties, stock options/ownership, or expert testimony for the last 12 months.

CRediT authorship contribution statement

Xianhua Han: Formal analysis, Writing - original draft. **Ping Wu:** Methodology, Writing - review & editing. **Ian Alberts:** Methodology, Software, Validation, Writing - original draft. **Hucheng Zhou:** Software, Visualization. **Huan Yu:** Data curation, Resources. **Panagiotis Bargiotas:** Methodology, Validation, Writing - review & editing. **Igor Yakushev:** Formal analysis, Validation, Writing - review & editing. **Jian Wang:** Data curation, Investigation, Resources. **Guenter Höglinger:** Supervision, Investigation, Writing - original draft. **Stefan Förster:** Supervision, Investigation. **Claudio Bassetti:** Supervision, Investigation. **Wolfgang Oertel:** Supervision, Funding acquisition, Investigation. **Markus Schwaiger:** Supervision, Investigation, Writing - original draft. **Sung-Cheng Huang:** Supervision, Investigation. **Paul Cumming:** Conceptualization, Supervision, Investigation. **Axel Rominger:** Supervision, Investigation. **Jiehui Jiang:** Conceptualization, Project administration, Resources, Writing - review & editing. **Chuantao Zuo:** Conceptualization, Data curation, Project administration, Funding acquisition, Resources. **Kuangyu Shi:** Conceptualization, Investigation, Project administration.

Acknowledgments

Wolfgang H Oertel is Hertie-Senior Research Professor supported by the Charitable Hertie Foundation, Frankfurt/Main, Germany. This study was supported by the National Science Foundation of China (grant numbers 81971641, 81671239, 81771483, 81401135, and 81361120393), the Sino-German Center for Research Promotion (GZ 1265, GZ 1510), 111 Project (D20031), and Shanghai Municipal Science and Technology Major Project (Grant No. 2017SHZDZX01); Science and Technology Commission of Shanghai Municipality (19441903500, 17JC1401600).

Appendix A. Supplementary data

Supplementary data to this article can be found online at https://doi.org/10.1016/j.nicl.2020.102294.

References

Boeve, B.F., 2010. REM sleep behavior disorder: updated review of the core features, the REM sleep behavior disorder-neurodegenerative disease association, evolving concepts, controversies, and future directions. Ann. New York Acad. Sci. 1184, 15–54. https://doi.org/10.1111/j.1749-6632.2009.05115.x. 2010/02/12.

Postuma, R.B., Gagnon, J.F., Vendette, M., et al., 2009. Quantifying the risk of neurodegenerative disease in idiopathic REM sleep behavior disorder. Neurology 72, 1296–1300. https://doi.org/10.1212/01.wnl.0000340980.19702.6e. 2008/12/26.

Iranzo, A., Tolosa, E., Gelpi, E., et al., 2013. Neurodegenerative disease status and post-mortem pathology in idiopathic rapid-eye-movement sleep behaviour disorder: an observational cohort study. Lancet Neurol. 12, 443–453. https://doi.org/10.1016/S1474-4422(13)70056-5. 2013/04/09.

Iranzo, A., Molinuevo, J.L., Santamaria, J., et al., 2006. Rapid-eye-movement sleep behaviour disorder as an early marker for a neurodegenerative disorder: a descriptive study. Lancet Neurol. 5, 572–577. https://doi.org/10.1016/s1474-4422(06)70476-8. 2006/06/20.

Galbiati, A., Verga, L., Giora, E., et al., 2019. The risk of neurodegeneration in REM sleep behavior disorder: a systematic review and meta-analysis of longitudinal studies. Sleep Med. Rev. 43, 37–46. https://doi.org/10.1016/j.smrv.2018.09.008. 2018/12/07.

Schenck, C.H., Boeve, B.F., Mahowald, M.W., 2013. Delayed emergence of a parkinsonian disorder or dementia in 81% of older men initially diagnosed with idiopathic rapid eye movement sleep behavior disorder: a 16-year update on a previously reported series. Sleep Med. 14, 744–748. https://doi.org/10.1016/j.sleep.2012.10.009. 2013/01/26.

Gagnon, J.F., Bedard, M.A., Fantini, M.L., et al., 2002. REM sleep behavior disorder and REM sleep without atonia in Parkinson's disease. Neurology 59, 585–589 2002/08/28.

Schrag, A., Horsfall, L., Walters, K., et al., 2015. Prediagnostic presentations of Parkinson's disease in primary care: a case-control study. Lancet Neurol. 14, 57–64. https://doi.org/10.1016/s1474-4422(14)70287-x. 2014/12/02.

Iranzo, A., Santamaria, J., Rye, D.B., et al., 2005. Characteristics of idiopathic REM sleep behavior disorder and that associated with MSA and PD. Neurology 65, 247–252. https://doi.org/10.1212/01.wnl.0000168864.97813.e0. 2005/07/27.

Nestor, P.J., Altomare, D., Festari, C., et al., 2018. Clinical utility of FDG-PET for the differential diagnosis among the main forms of dementia. Eur. J. Nucl. Med. Mol. Imaging 45, 1509–1525 2018/05/0810.1007/s00259-018-4035-y.

Drzezga, A., Altomare, D., Festari, C., et al., 2018. Diagnostic utility of 18F-Fluorodeoxyglucose positron emission tomography (FDG-PET) in asymptomatic subjects at increased risk for Alzheimer's disease. Eur. J. Nucl. Med. Mol. Imaging 45. https://doi.org/10.1007/s00259-018-4032-1.

Eidelberg, D., 1992. Positron emission tomography studies in parkinsonism. Neurol. Clin. 10.

Borghammer, P., Chakravarty, M., Jonsdottir, K.Y., et al., 2010. Cortical hypometabolism and hypoperfusion in Parkinson's disease is extensive: probably even at early disease stages. Brain Struct. Function. https://doi.org/10.1007/s00429-010-0246-0.

Meles, S.K., Teune, L.K., de Jong, B.M., et al., 2017. Metabolic imaging in Parkinson disease. J. Nucl. Med. : Off. Publ., Soc. Nucl. Med. 58, 23–28. https://doi.org/10.2967/jnumed.116.183152. 2016/11/24.

Ge, J., Wu, P., Peng, S., et al., 2015. Assessing cerebral glucose metabolism in patients with idiopathic rapid eye movement sleep behavior disorder. J. Cereb. Blood Flow Metab. 35, 2062–2069. https://doi.org/10.1038/jcbfm.2015.173. 2015/07/30.

Teune, L.K., Bartels, A.L., de Jong, B.M., et al., 2010. Typical cerebral metabolic patterns in neurodegenerative brain diseases. Movement Disord. 25, 2395–2404. https://doi.org/10.1002/mds.23291. 2010/07/30.

Yong, S.W., Yoon, J.K., An, Y.S., et al., 2007. A comparison of cerebral glucose metabolism in Parkinson's disease, Parkinson's disease dementia and dementia with Lewy bodies. Eur. J. Neurol. 14, 1357–1362. https://doi.org/10.1111/j.1468-1331.2007.01977.x.

Borghammer, P., Cumming, P., Aanerud, J., et al., 2009. Subcortical elevation of metabolism in Parkinson's disease–a critical reappraisal in the context of global mean normalization. NeuroImage 47, 1514–1521. https://doi.org/10.1016/j.neuroimage.2009.05.040.

Eidelberg, D., 2009. Metabolic brain networks in neurodegenerative disorders: a functional imaging approach. Trends Neurosci. 32. https://doi.org/10.1016/j.tins.2009.06.003.

Eckert, T., Tang, C., Ma, Y., et al., 2008. Abnormal metabolic networks in atypical parkinsonism. Movement Disord. 23. https://doi.org/10.1002/mds.21933.

Ma, Y., Tang, C., Spetsieris, P.G., et al., 2007. Abnormal metabolic network activity in Parkinson's disease: test-retest reproducibility. J. Cerebral Blood Flow Metab. 27, 597–605. https://doi.org/10.1038/sj.jcbfm.9600358. 2006/06/29.

Tang, C.C., Poston, K.L., Eckert, T., et al., 2010. Differential diagnosis of parkinsonism: a metabolic imaging study using pattern analysis. Lancet Neurol. 9, 149–158. https://doi.org/10.1016/s1474-4422(10)70002-8. 2010/01/12.

Wu, P., Wang, J., Peng, S., et al., 2013. Metabolic brain network in the Chinese patients with Parkinson's disease based on 18F-FDG PET imaging. Parkinsonism Related Disord. 19, 622–627. https://doi.org/10.1016/j.parkreldis.2013.02.013. 2013/03/27.

Niethammer, M., Eidelberg, D., 2012. Metabolic brain networks in translational neurology: concepts and applications. Ann. Neurol. 72. https://doi.org/10.1002/ana.23631.

Hughes, A.J., Daniel, S.E., Kilford, L., et al., 1992. Accuracy of clinical diagnosis of idiopathic Parkinson's disease: a clinico-pathological study of 100 cases. J. Neurol. Neurosurg. Psychiatry 55.

Duchna, H.W., 2006. Sleep-related breathing disorders–a second edition of the International Classification of Sleep Disorders (ICSD-2) of the American Academy of Sleep Medicine (AASM). Pneumologie (Stuttgart, Germany) 60, 568–575. https://doi.org/10.1055/s-2006-944248.

Montplaisir, J., Gagnon, J.F., Fantini, M.L., et al., 2010. Polysomnographic diagnosis of idiopathic REM sleep behavior disorder. Movement Disord. (2010/09/08), 2044–2051. https://doi.org/10.1002/mds.23257.

Zhang, H., Wu, P., Ziegler, S.I., et al., 2017. Data-driven identification of intensity normalization region based on longitudinal coherency of (18)F-FDG metabolism in the healthy brain. NeuroImage 146. https://doi.org/10.1016/j.neuroimage.2016.09.031.

Wu, P., Yu, H., Peng, S., et al., 2014. Consistent abnormalities in metabolic network activity in idiopathic rapid eye movement sleep behaviour disorder. Brain J. Neurol. 137, 3122–3128. https://doi.org/10.1093/brain/awu290. 2014/10/24.

Postuma, R.B., Arnulf, I., Hogl, B., et al., 2012. A single-question screen for rapid eye movement sleep behavior disorder: a multicenter validation study. Movement Disord. 27. https://doi.org/10.1002/mds.25037.

Tzourio-Mazoyer, N., Landeau, B., Papathanassiou, D., et al., 2002. Automated anatomical labeling of activations in SPM using a macroscopic anatomical parcellation of the MNI MRI single-subject brain. NeuroImage 15: 273–289. https://doi.org/10.1006/nimg.2001.0978.

Huang, Z., Jiang, C., Li, L., et al., 2019. Correlations between dopaminergic dysfunction and abnormal metabolic network activity in REM sleep behavior disorder. J. Cereb. Blood Flow Metab. https://doi.org/10.1177/0271678x19828916.

Meles, S.K., Renken, R.J., Janzen, A., et al., 2018. . The metabolic pattern of idiopathic REM sleep behavior disorder reflects early-stage Parkinson disease. J. Nucl. Med. 59, 1437–1444. https://doi.org/10.2967/jnumed.117.202242. 2018/02/25.

Arnaldi, D., Meles, S.K., Giuliani, A., et al., 2019. Brain glucose metabolism heterogeneity in idiopathic REM sleep behavior disorder and in Parkinson's disease. J. Parkinson's Dis. 9, 229–239. https://doi.org/10.3233/jpd-181468. 2019/02/12.

Vendette, M., Montplaisir, J., Gosselin, N., et al., 2012. Brain perfusion anomalies in rapid eye movement sleep behavior disorder with mild cognitive impairment. Movement Disord. 27, 1255–1261. https://doi.org/10.1002/mds.25034.

Mentis, M.J., McIntosh, A.R., Perrine, K., et al., 2002. Relationships among the metabolic patterns that correlate with mnemonic, visuospatial, and mood symptoms in Parkinson's disease. Am. J. Psychiatry 159. https://doi.org/10.1176/appi.ajp.159.5.746.

Colloby, S.J., Fenwick, J.D., Williams, E.D., et al., 2002. A comparison of (99m)Tc-HMPAO SPET changes in dementia with Lewy bodies and Alzheimer's disease using statistical parametric mapping. Eur. J. Nucl. Med. Molecular Imaging 29. https://doi.org/10.1007/s00259-002-0778-5.

Vendette, M., Gagnon, J.F., Soucy, J.P., et al., 2011. Brain perfusion and markers of neurodegeneration in rapid eye movement sleep behavior disorder. Movement Disord. 26, 1717–1724. https://doi.org/10.1002/mds.23721.

Sakurai, H., Hanyu, H., Inoue, Y., et al., 2014. Longitudinal study of regional cerebral blood flow in elderly patients with idiopathic rapid eye movement sleep behavior disorder. Geriatr. Gerontol. Int. 14, 115–120. https://doi.org/10.1111/ggi.12068.

Ota, K., Fujishiro, H., Kasanuki, K., et al., 2016. Prediction of later clinical course by a specific glucose metabolic pattern in non-demented patients with probable REM sleep behavior disorder admitted to a memory clinic: a case study. Psychiatry Res. Neuroimaging 248, 151–158. https://doi.org/10.1016/j.pscychresns.2015.12.004.

Ma, Y., Tang, C., Moeller, J.R., et al., 2009. Abnormal regional brain function in Parkinson's disease: truth or fiction? NeuroImage 45, 260–266. https://doi.org/10.1016/j.neuroimage.2008.09.052.

Borghammer, P., Cumming, P., Aanerud, J., et al., 2009. Artefactual subcortical hyperperfusion in PET studies normalized to global mean: lessons from Parkinson's disease. NeuroImage 45, 249–257. https://doi.org/10.1016/j.neuroimage.2008.07.042.